

Ulrich Rester,^{a*†} Wolfram Bode,^a Claudio A. M. Sampaio,^b Ennes A. Auerswald^{c,d} and Alexandre P. Y. Lopes^{c,e}

^aMax-Planck-Institut für Biochemie, Abteilung Strukturforchung, Am Klopferspitz 18a, 82152 Martinsried, Germany, ^b UNIFESP-EPM, Departamento de Bioquímica, São Paulo, SP, Brazil, ^cLudwig-Maximilians-Universität München, Abteilung für Klinische Chemie und Klinische Biochemie, Klinikum der Universität – Innenstadt, Nussbaumstrasse 20, 80336 München, Germany, ^dKlinikum der Universität München, Neurologische Klinik und Poliklinik – Grosshadern, Marchionistrasse 15, 81377 München, Germany, and ^eInstituto Butantan, Centro de Biotecnologia, Av. Vital Brasil 1500, CEP 05503-900, São Paulo, SP, Brazil

† Present address: CallistoGen AG, Neuendorfstrasse 24b, 16761 Hennigsdorf (b. Berlin), Germany.

Correspondence e-mail: ulrich.rester@callistogen.com

Cloning, purification, crystallization and preliminary X-ray diffraction analysis of the antistasin-type inhibitor ghilanten (domain I) from *Haementeria ghilianii* in complex with porcine β -trypsin

Received 22 January 2001

Accepted 1 May 2001

Ghilanten, isolated from the leech *Haementeria ghilianii*, is a potent two-domain anticoagulant protein homologous to the factor Xa inhibitor antistasin. A synthetic gene encoding the amino-terminal domain of ghilanten (ghilanten-D1) was constructed, expressed in the methylotrophic yeast *Pichia pastoris* and purified by heparin-Sepharose chromatography. Recombinant ghilanten-D1 inhibits bovine trypsin and human factor Xa with equilibrium inhibition constants (K_i) of 126 and 1.2 nM, respectively. Ghilanten-D1 has been crystallized in complex with porcine β -trypsin; three different-looking but isomorphous crystal forms were obtained, each belonging to the orthorhombic space group $P2_12_12_1$. These crystals diffracted to beyond 3.6 Å resolution using a rotating-anode X-ray source. A data set complete to 3.7 Å resolution was collected.

1. Introduction

Haemostasis is the delicate balance between the processes of coagulation, anticoagulation and fibrinolysis. The coagulation factor Xa, responsible for the activation of prothrombin to α -thrombin, plays a strategic role in the intrinsic and extrinsic coagulation pathways (Davie *et al.*, 1991). Antigenic and functional deficiencies of factor X result in moderate to severe bleeding diatheses (Watzke *et al.*, 1990, 1991). Moreover, factor Xa contributes to the pathogenicity of certain influenza virus strains *via* activation of viral glycoproteins necessary for cell invasion (Suzuki *et al.*, 1991).

The inactive zymogen factor X circulates in the blood as a disulfide-linked two-chain molecule (139 amino-acid light chain, 303 amino-acid heavy chain; MW 59 000 Da). The catalytic domain exhibits a high degree of sequence homology with other trypsin-like serine proteinases (Davie *et al.*, 1979; Furie & Furie, 1988) and an active-site cleft similar to those of trypsin and chymotrypsin (Padmanabhan *et al.*, 1993).

Because of its pivotal position in blood coagulation, the selective inhibition of factor Xa represents a primary target for anti-coagulant therapy. Factor Xa is inhibited endogenously by antithrombin III, α_1 -proteinase inhibitor, α_2 -macroglobulin and tissue-factor pathway inhibitor TFPI (Broze, 1995). It can also be blocked by the haemato-phage-derived proteins tick anticoagulant peptide (TAP; Waxman *et al.*, 1990) and antistasin (ATS; Tuszyński *et al.*, 1987), by the antistasin-related peptides (Ohta *et al.*, 1994),

by the antistasin-type inhibitor Yagin (Werber *et al.*, 1995) and by the five sequence-related variants of ghilanten (Condra *et al.*, 1989).

The most potent isoform of the ghilantens, generally referred to as ghilanten, is a disulfide cross-linked 119 amino-acid protein with anticoagulant and antimetastatic properties (Brankamp *et al.*, 1990; Blankenship *et al.*, 1990). Ghilanten has been expressed recently in the methylotrophic yeast *Pichia pastoris* (Brankamp *et al.*, 1995). Its primary structure reveals a twofold internal repeat (Fig. 1) consisting of the amino-terminal domain, blocking the active site of factor Xa (Brankamp *et al.*, 1990), and the carboxy-terminal domain, which presents a heparin-binding region (residues 93–119) and possibly mediates interactions with heparan sulfate proteoglycans on the arterial wall (Brankamp *et al.*, 1991). Ghilanten shows almost 90% sequence identity with antistasin, the prototype of the antistasin-type inhibitor family, indicating minimal evolutionary divergence from a common ancestral inhibitor (Condra *et al.*, 1989).

As part of an ongoing study aimed at understanding the inhibitory mechanism of antistasin-type inhibitors, we have commenced the determination of the three-dimensional structure of β -trypsin in complex with the amino-terminal domain of ghilanten (residues 1–55). In this paper, we present the over-expression of ghilanten-D1 in *P. pastoris* and an efficient purification protocol. Furthermore, the crystallization and preliminary X-ray diffraction analysis of the complex formed with porcine β -trypsin is described.

2. Materials and methods

2.1. Cloning of the amino-terminal domain of the ghilanten gene fragment (ghilanten-D1)

All DNA manipulations were carried out using standard procedures (Sambrook *et al.*, 1989). A synthetic gene encoding the amino-terminal domain of ghilanten (ghilanten-D1) was designed and constructed (Lopes, 2000). The synthetic gene was ligated into the pUC19 vector (Amersham) cut with *EcoRI* and *HindIII* and then used for transforming TG1 *Escherichia coli* cells. After confirming the sequence, the ghilanten-D1 gene was excised as a *XhoI* (5') and *EcoRI* (3') fragment and ligated into the expression vector pPIC9 (Invitrogen) in frame with the DNA sequence encoding the α -mating pre-pro secretion signal of *S. cerevisiae*. The host *P. pastoris* strain KM71 (Invitrogen) was transformed by electroporation with ~5 μ g of the linearized (*Sall*) pPIC9 vector for integration at the *his4* locus. Transformants were selected by conversion of *his4* for HIS4 phenotype.

2.2. Expression and purification of ghilanten-D1

20 individual colonies of the transformed *P. pastoris* strain KM71 (pPIC9 construct) were grown at 303 K to an OD₆₀₀ of 1.3–1.5 in 50 ml BMGY medium [1%(v/v) glycerol, 2%(w/v) peptone, 1%(w/v) yeast extract, 1.3%(w/v) yeast nitrogen base without

amino acids, 0.004(w/v) biotin and 10%(v/v) potassium phosphate buffer (1 M, pH 6.0)] and tested for human factor Xa inhibitory activity. One high-expressing colony was raised in 11 BMGY medium, cells were harvested (4000g) and resuspended in 200 ml BMBC medium [1%(v/v) methanol, 2%(w/v) casamino acids, 1.3%(w/v) yeast nitrogen base without amino acids, 0.004(w/v) biotin and 10%(v/v) potassium phosphate buffer (1 M, pH 6.0)]. The culture was induced by addition of 0.5%(v/v) methanol per day and cultured for 72 h.

The supernatant was collected (4000g), concentrated to 30–50 ml (YM3 Diaflo membrane, Amicon) and equilibrated to 0.02 M potassium phosphate pH 6.0. The two subsequent tandem chromatographic steps were conducted with a prepacked heparin-Sepharose column (5 ml HiTrap column, FPLC, Pharmacia Biotech) as suggested by the manufacturer. The bound proteins were eluted with a linear gradient of 0–1 M NaCl in the equilibration buffer. The efflux was fractionated and checked for inhibitory activity. Peak fractions were pooled and analysed by SDS–PAGE (Laemmli, 1970).

2.3. Determination of equilibrium dissociation constants (*K_i*) for trypsin and factor Xa

The equilibrium dissociation constants (*K_i*) of the complexes between ghilanten-D1 and either bovine β -trypsin (Merck) or

human factor Xa (Enzyme Research Laboratories) were determined using the method of Bieth (1980). Briefly, trypsin (100 nM) or factor Xa (100 pM) were incubated (30 min) with different ghilanten-D1 concentrations in 0.02 M Tris–HCl, 0.15 M NaCl, 0.01% Triton X-100 pH 8.0 (trypsin) or pH 7.4 (factor Xa) at 310 K. The residual enzyme activities were measured by adding the substrates L-BAPA (Merck) for trypsin and Boc-IEGR-AMC (Bachem) for factor Xa. Apparent *K_i* values were calculated by fitting the steady-state velocities to the equation for tight-binding inhibitors using a non-linear regression analysis (Morrison, 1969).

2.4. Crystallization and preliminary X-ray analysis

Lyophilized porcine pancreatic trypsin type IX (Sigma) was inhibited by a slight molar excess of recombinant ghilanten-D1 in 100 mM NaCl, 50 mM MES pH 6.5 for 1 h at 277 K, concentrated to 7.5 mg ml⁻¹ protein by use of Microsep 3K tubes (Filtron), dialyzed against 150 mM NaCl, 20 mM MES pH 6.5 and filtered (0.22 μ m Ultrafree-MC, Millipore). Crystallization trials were set up as vapour-diffusion experiments at 293 K using the sitting-drop method (McPherson, 1989). Crystallization conditions were screened using the multifactorial crystal screen (Hampton Research). Initial successful crystallization conditions were further optimized.

Crystals were mounted in thin-walled glass capillaries and checked for X-ray diffraction. Diffraction data were collected at 291 K with a 30 cm MAR Research imaging-plate detector system equipped with a Rigaku RU-200 rotating-anode generator (Rigaku, Japan) producing

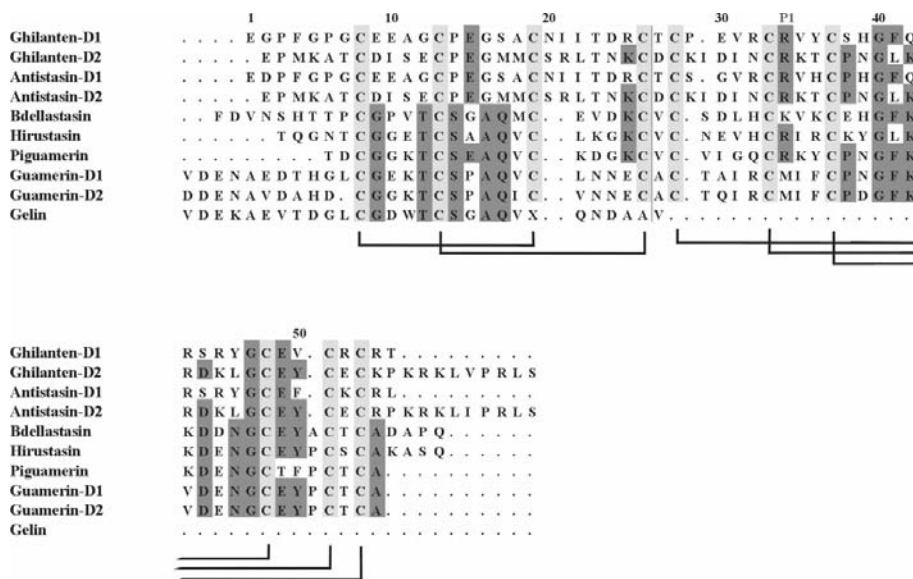


Figure 1 Sequence comparison of the antistatin-type inhibitors (Condra *et al.*, 1989), antistatin (Nutt *et al.*, 1988), bdeIIastasin (Moser *et al.*, 1998), hirustasin (Söllner *et al.*, 1994), piguamerin (Kim & Kang, 1998), guamerin (Jung *et al.*, 1995) and the amino-terminal residues of gelin (Electricwala *et al.*, 1993). D1 and D2 indicate the amino-terminal and the carboxy-terminal domain of the inhibitors, respectively. Black lines display the disulfide connectivity.

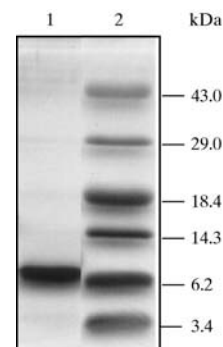


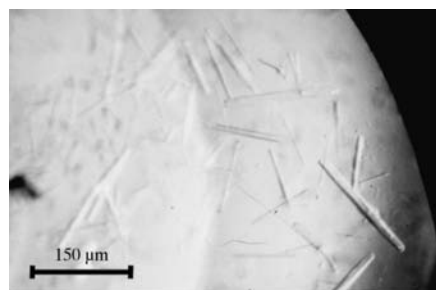
Figure 2 Coomassie-stained SDS–PAGE (15%) showing the product of the preparation of the amino-terminal domain of ghilanten (ghilanten-D1). Lane 1, purified ghilanten-D1; lane 2, molecular-weight markers (BRL).

graphite-monochromated Cu $K\alpha$ radiation ($\lambda = 1.5418 \text{ \AA}$) at 50 kV and 100 mA. The images were processed using the *MOSFLM* package (Leslie, 1994) and the data were scaled and merged with routines implemented in the *CCP4* program suite (1994). Self-rotation functions were calculated with the program *GLRF* (Tong & Rossmann, 1990).

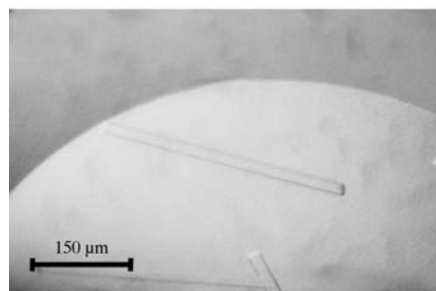
3. Results and discussion

3.1. Cloning, expression and purification of the amino-terminal domain of ghilanten (ghilanten-D1)

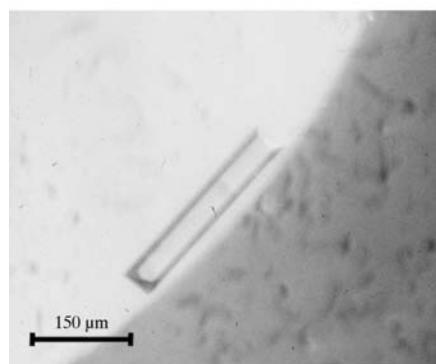
Based on the ghilanten amino-acid sequence (Blankenship *et al.*, 1990; see also Fig. 1), a synthetic gene of the amino-terminal domain of ghilanten was constructed



(a)



(b)



(c)

Figure 3

Crystals of the porcine β -trypsin-ghilanten-D1 complex. Crystallization setup as described in the text. Note the influence of the MPD concentration, pH and additives. The three photographs are on the same scale.

and the vector pPIC9 was used for expression in the methylotrophic yeast *P. pastoris* strain KM71. The amount secreted into the medium was calculated to be 8.2 mg l^{-1} as judged by its factor Xa inhibition activity.

Although the heparin-binding region of ghilanten is believed to be located in the carboxy-terminal domain (Brankamp *et al.*, 1991), purification on heparin-Sepharose was used for the amino-terminal domain of ghilanten-D1 (Palladino *et al.*, 1991). Based on this result, two heparin-Sepharose chromatography steps were used for the purification of ghilanten-D1. 7–8 mg of highly purified protein per liter of supernatant was obtained routinely as judged by SDS-PAGE (Fig. 2) and reverse-phase HPLC analysis (data not shown).

The inhibitory activity of the recombinant protein was determined by enzymatic inhibition tests, revealing equilibrium dissociation constants (K_i values) for the human factor Xa-ghilanten-D1 complex and the bovine β -trypsin-ghilanten-D1 complex of 1.2 and 126 nM, respectively. The K_i value found for the human factor Xa-ghilanten-D1 complex is similar to the K_i value (1.7 nM) described for the complex of factor Xa with the amino-terminal domain of antistasin.

3.2. Crystallization

The initial crystallization trials resulted in one promising crystallization condition with 4 μl droplets [3 μl protein solution (7.5 mg ml^{-1}) plus 1 μl reservoir solution] against 1 ml of reservoir solution [100 mM HEPES pH 7.5, 70% (v/v) MPD, 600 mM $(\text{NH}_4)_2\text{SO}_4$]. Many small needles appeared after one week (Fig. 3a). The largest of these crystals, with approximate dimensions of $150 \times 10 \times 10 \text{ \mu m}$, did not show any reflections in X-ray diffraction experiments. Therefore, the initial needles were further optimized. The first diffracting β -trypsin-ghilanten-D1 crystals (GD-I) appeared after four weeks from phase separation. These stick-shaped crystals diffracted to about 3.6 \AA resolution. Unfortunately, microseeding and macroseeding did not speed up the crystallization process.

Crystallization experiments with a lower precipitant ratio [40% (v/v) and 30% (v/v) MPD] led to fewer but larger crystals. Stick-shaped GD-II crystals (Fig. 3b) and rod-shaped GD-III crystals (Fig. 3c) grew to maximum dimensions of $400 \times 20 \times 20 \text{ \mu m}$ and $300 \times 40 \times 40 \text{ \mu m}$, respectively. The detailed crystallization conditions and the crystal properties are summarized in Table 1.

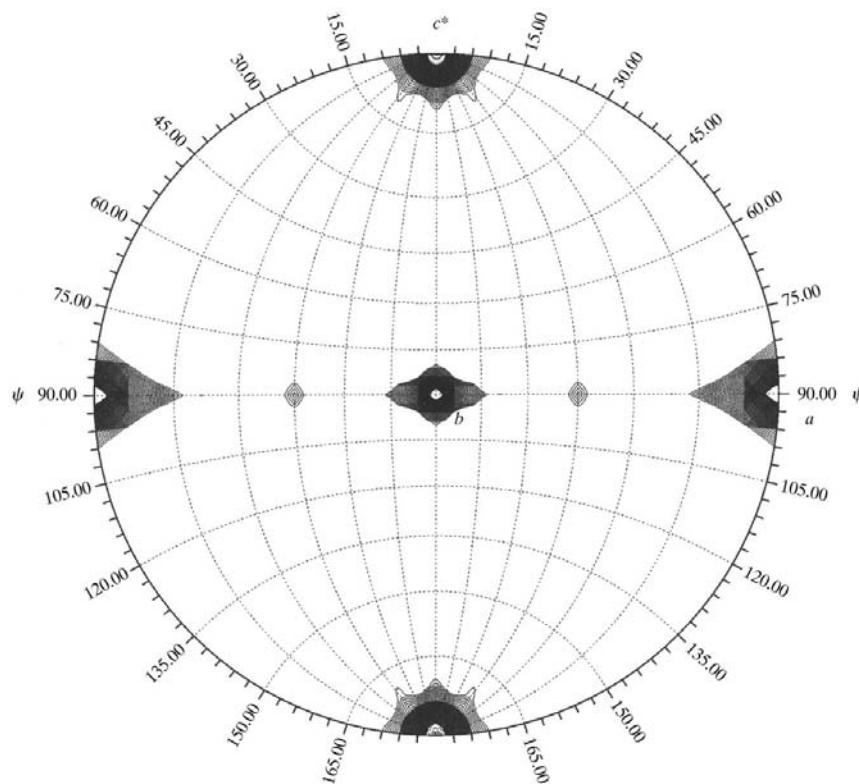


Figure 4

Result from a locked self-rotation function calculated for a twofold correlation ($\kappa = 180^\circ$) contoured with a 2.0σ cutoff (polar convention XZK, orthogonalization AXABZ according to *GLRF*; Tong & Rossmann, 1990). The peak at $\Phi = 45^\circ$, $\Psi = 90^\circ$ and $\kappa = 180^\circ$ clearly indicates the presence of a twofold NCS axis located between the *a* and *b* axes, oriented perpendicular to the crystallographic twofold axis.

Table 1

Crystallization conditions and crystal properties of the porcine β -trypsin–ghilanten-D1 complex.

The values in parentheses correspond to the highest resolution shell: 3.79–3.60 Å for GD-I, 4.11–3.90 Å for GD-II and 3.79–3.60 Å for GD-III.

	GD-I	GD-II	GD-III
Precipitant	70% (v/v) MPD, 600 mM (NH ₄) ₂ SO ₄	40% (v/v) MPD, 600 mM (NH ₄) ₂ SO ₄	30% (v/v) MPD, 600 mM (NH ₄) ₂ SO ₄
Buffer	100 mM HEPES	100 mM HEPES	100 mM Na cacodylate
pH	7.2	7.5	6.5
Additives	—	200 mM Na citrate	200 mM Mg acetate
Time	4 weeks	14 months	18 months
Morphology	Needles	Sticks	Rods
Dimensions (mm)	0.80 × 0.045 × 0.040	0.70 × 0.035 × 0.035	0.30 × 0.060 × 0.040
Unit-cell parameters (Å)			
<i>a</i>	62.37	62.09	62.03
<i>b</i>	102.71	102.14	101.99
<i>c</i>	117.72	118.20	117.65
Space group	<i>P</i> 2 ₁ 2 ₁ 2 ₁	<i>P</i> 2 ₁ 2 ₁ 2 ₁	<i>P</i> 2 ₁ 2 ₁ 2 ₁
Oscillation angle per frame (°)	1	2	1
X-ray time exposure (s per frame)	1200	3600	1200
Number of frames	45	10	30
Diffraction limit (Å)	3.6	3.9	3.6
No. of accepted reflections	15740	5487	10007
No. of unique reflections	5402	3143	6142
Overall multiplicity	2.9	1.7	1.6
Completeness (%)	59.1 (61.7)	45.3 (74.0)	69.8 (73.4)
<i>R</i> _{merge} [†] (%)	26.7 (47.0)	24.0 (34.8)	22.1 (35.1)

[†] $R_{\text{merge}} = \sum_{hkl} [(\sum_i |I_i - \langle I \rangle|) / \sum_i I_i]$ for equivalent observations.

Table 2

Data-processing statistics (GD-I/II/III).

Values in parentheses correspond to the highest resolution shell, 3.90–3.70 Å.

Space group	<i>P</i> 2 ₁ 2 ₁ 2 ₁
Unit-cell parameters (Å)	
<i>a</i>	62.37
<i>b</i>	102.71
<i>c</i>	117.72
Unit-cell volume (Å ³)	754117
<i>V</i> _M (Å ³ Da ⁻¹)	3.19 (61% H ₂ O)
Asymmetric unit content	2 complexes
Limiting resolution (Å)	3.7
No. of crystals used	3
No. of significant measurements	25954
No. of independent reflections	7853
Completeness of data (%)	93.4 (95.7)
Overall multiplicity (%)	3.3 (3.3)
Average <i>R</i> _{merge} [†]	0.299 (0.453)

[†] $R_{\text{merge}} = \sum_{hkl} [(\sum_i |I_i - \langle I \rangle|) / \sum_i I_i]$ for equivalent observations.

3.3. Crystallographic characterization

Preliminary X-ray data were collected from representative single crystals obtained at three different crystallization conditions. The crystallographic parameters listed in Table 1 represent the results obtained from these X-ray diffraction experiments. None of the isomorphous crystals were stable for long in the X-ray beam. Soaking the crystals in cryobuffers containing increased amounts of precipitant led to non-diffracting crystals.

A data set complete to 3.7 Å resolution was collected from three isomorphous crys-

tals. The detailed data-processing statistics are summarized in Table 2. Locked Patterson self-rotation function calculations indicate the presence of a twofold NCS axis (Fig. 4). A Patterson search and consideration of the Matthews parameter ($V_M = 3.19 \text{ \AA}^3 \text{ Da}^{-1}$, solvent content 61%) suggest the likely presence of two porcine β -trypsin–ghilanten-D1 complexes in the asymmetric unit.

The financial support (to UR) provided by Callistogen AG is gratefully acknowledged.

References

Bieth, J. G. (1980). *Bull. Eur. Physiopathol. Respir.* **16**, 183–195.

Blankenship, D. T., Brankamp, R. G., Manley, G. D. & Cardin, A. D. (1990). *Biochem. Biophys. Res. Commun.* **166**, 1384–1389.

Brankamp, R. G., Blankenship, D. T., Sunkara, P. S. & Cardin, A. D. (1990). *Lab. Clin. Med.* **115**, 89–97.

Brankamp, R. G., Manley, G. G., Blankenship, D. T., Bowlin, T. L. & Cardin, A. D. (1991). *Blood Coagul. Fibrinolysis*, **2**, 161–166.

Brankamp, R. G., Sreekrishna, K., Smith, P. L., Blankenship, D. T. & Cardin, A. D. (1995). *Protein Expr. Purif.* **6**, 813–820.

Broze, G. J. (1995). *Thromb. Haemost.* **74**, 90–93. Collaborative Computational Project, Number 4 (1994). *Acta Cryst.* **D50**, 760–763.

Condra, C., Nutt, E., Petroski, C. J., Simpson, E., Friedman, P. A. & Jacobs, J. W. (1989). *Thromb. Haemost.* **61**, 437–441.

Davie, E. W., Fujikawa, K. & Kisiel, W. (1991). *Biochemistry*, **30**, 10363–10370.

Davie, E. W., Fujikawa, K., Kurachi, K. & Kisiel, W. (1979). *Adv. Enzymol.* **48**, 277–318.

Electricwala, A., von Sicard, N. A. E., Sawyer, R. T. & Atkinson, T. (1993). *J. Enzyme Inhib.* **6**, 293–302.

Furie, B. & Furie, B. C. (1988). *Cell*, **53**, 505–518.

Jung, H. I., Kim, S. I., Ha, K. S., Joe, C. O. & Kang, K. W. (1995). *J. Biol. Chem.* **270**, 13879–13884.

Kim, D. R. & Kang, K. W. (1998). *Eur. J. Biochem.* **254**, 692–697.

Laemmli, U. K. (1970). *Nature (London)*, **227**, 680–685.

Leslie, A. G. W. (1994). *MOSFLM User Guide, MOSFLM Version 5.23*. Cambridge: MRC Laboratory of Molecular Biology.

Lopes, A. P. Y. (2000). *Structural and Functional Studies on the Protease Inhibitors Bdelastasin and Ghilanten of the Antistasin Family*. São Paulo, Brazil: University of Sao Paulo.

McPherson, A. (1989). Editor. *Preparation and Analysis of Protein Crystals*. Malabar, Florida, USA: Krieger Publishing Co.

Morrison, J. F. (1969). *Biophys. Acta*, **185**, 269–286.

Moser, M., Auerswald, E., Mentele, R., Eckerskorn, C., Fritz, H. & Fink, E. (1998). *Eur. J. Biochem.* **253**, 212–220.

Nutt, E., Gasic, T., Rodkey, J., Gasic, G. J., Jacobs, J. W., Friedman, P. A. & Simpson, E. (1988). *J. Biol. Chem.* **263**, 10162–10167.

Ohta, N., Brush, M. & Jacobs, J. W. (1994). *Thromb. Haemost.* **72**, 825–830.

Padmanabhan, K., Padmanabhan, K. T., Tulinsky, A., Park, C. H., Bode, W., Huber, R., Blankenship, D. T., Cardin, A. D. & Kisiel, W. (1993). *J. Biol. Chem.* **268**, 947–966.

Palladino, L. O., Tung, J. S., Dunwiddie, C., Alves, K., Lenny, A. B., Przysocki, C., Lehman, D., Nutt, E., Cuca, G. C., Law, S. W., Silberklang, M., Ellis, R. W. & Mark, G. E. (1991). *Protein Expr. Purif.* **2**, 37–42.

Sambrook, J., Fritsch, E. F. & Maniatis, T. (1989). *Molecular Cloning: A Laboratory Manual*, Vol. 1–3, edited by C. Nolan. Cold Spring Harbor, NY, USA: Cold Spring Harbor Laboratory Press.

Söllner, C., Mentele, R., Eckerskorn, C., Fritz, H. & Sommerhoff, C. P. (1994). *Eur. J. Biochem.* **219**, 937–943.

Suzuki, H., Harada, A., Hayashi, Y., Wada, K., Asaka, J., Gotoh, B., Ogasawara, T. & Nagai, Y. (1991). *FEBS Lett.* **283**, 281–285.

Tong, L. & Rossmann, M. G. (1990). *Acta Cryst.* **A46**, 783–792.

Tuszynski, G. P., Gasic, T. B. & Gasic, G. J. (1987). *J. Biol. Chem.* **262**, 9718–9723.

Watzke, H. H., Lechner, K., Roberts, H. R., Reddy, S. V., Welsch, D. J., Friedman, P., Mahr, G., Jagadeeswaran, P., Monroe, D. M. & High, K. A. (1990). *J. Biol. Chem.* **265**, 11982–11989.

Watzke, H. H., Wallmark, A., Hamaguchi, N., Giardina, P., Stafford, D. W. & High, K. A. (1991). *J. Clin. Invest.* **88**, 1685–1689.

Waxman, L., Smith, D. E., Arcuri, K. E. & Vlasuk, G. P. (1990). *Science*, **248**, 593–596.

Werber, M. M., Zeelon, E., Levanon, A., Goldberg, M., Greenstein, L. A., Haim, B., Ashkenazi, S., Gelbart, H., Rigbi, M., Ezov, N., Nimrod, A., Parizada, B., Panet, A., Hanson, S. R. & Gorcki, M. (1995). *Thromb. Haemost.* **73**, 1312.